ACS APPLIED MATERIALS & INTERFACES

Research Article

www.acsami.org

Antibacterial Composite Film-Based Triboelectric Nanogenerator for Harvesting Walking Energy

Guang Qin Gu,[†,‡,∥] Chang Bao Han,[†,∥] Jing Jing Tian,[†,‡,∥] Cun Xin Lu,[†,‡] Chuan He,[†] Tao Jiang,[†] Zhou Li,[*,†] and Zhong Lin Wang[*,†,§]

[†]Beijing Institute of Nanoenergy and Nanosystems, Chinese Academy of Sciences, National Center for Nanoscience and Technology (NCNST), Beijing 100083, China

[‡]University of Chinese Academy of Sciences, Beijing 100049, China

[§]School of Materials Science and Engineering, Georgia Institute of Technology, Atlanta, Georgia 30332-0245, United States

ABSTRACT: As a green and eco-friendly technology, triboelectric nanogenerator (TENG) can harvest energy from human motion to generate electricity, so TENGs have been widely applied in wearable electronic devices to replace traditional batteries. However, the surface of these TENGs is easily contaminated and breeds bacteria, which is a threat to human health. Here, we report an antibacterial composite film-based triboelectric nanogenerator (ACF-TENG) that uses Ag-exchanged zeolite (Ag-zeolite) and polypropylene (PP) composite film as the triboelectric layer. Adding a small amount of Ag-zeolite with excellent antibacterial properties can increase the dielectric permittivity and improve the surface charge density of composite films, which enhances the output performance of the ACF-TENG. The open-circuit voltage (V_{OC}), short-circuit current (I_{SC}), and transferred charge (Q_{Tr}) of the ACF-TENG are about 193.3, 225.4, and 233.3% of those of a pure PP film-based TENG, respectively. Because of the silver in the Ag-zeolite, the ACF-TENG can effectively kill *Escherichia coli* and fungi. When used in insoles, the ACF-TENG can resist the athlete's foot fungus effectively and work as a power source to light up light-emitting diodes and charge capacitors. The ACF-TENG has wide application prospects in self-powered medical and healthcare electronics.

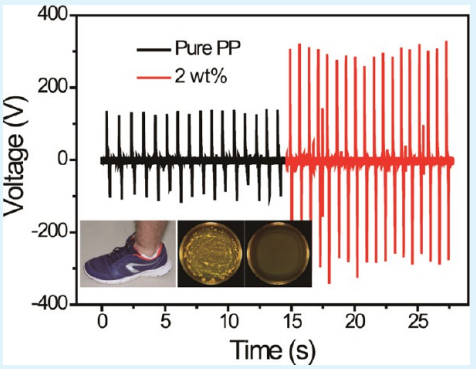

KEYWORDS: *triboelectric nanogenerator, polypropylene, antibacterial, silver-exchanged zeolite, composite film, walking-energy harvesting*

1. INTRODUCTION

Triboelectric nanogenerators (TENGs) can directly convert mechanical energies harvested from wind,[1−4] flowing water,[5−7] and human motion[8−10] into electricity on the basis of triboelectricity and the electrostatic induction effect. Since the first report in 2012,[11] TENGs have been widely utilized in various applications, such as energy harvesters,[8,12] detectors,[13,14] and self-powered sensors.[2,5,15] Among these applications, the integration of TENGs in wearable devices[16,17] or implantable devices[10] is of great interest because of their potential in powering portable devices. However, bacterial contamination of the TENGs in these applications is a huge concern because it poses a threat to human health. In this regard, exploration of TENGs with antibacterial properties is urgently needed for human health.

As a thermoplastic crystalline polymer, polypropylene (PP) is biocompatible, nontoxic, and cost-effective; therefore, it has been extensively applied in food packaging, medical delivery systems, carpets, fibers, toys, and so forth.[18] However, the surface of pure PP can get easily contaminated under certain temperature and humidity conditions. It is reported that adding nanoparticles is an effective way to offer the functionally of polymer materials.[19] In the PP matrix, nanoscale zinc oxide (ZnO),[19−22] titanium dioxide (TiO_2),[23] silver (Ag),[24,25] and copper (Cu)[26] are most commonly used as antibacterial fillers, but these metal ions are quickly released into the PP matrix. Thus, they are not suitable for long-term antibacterial usage.

For slow release of the metal ions into other materials, loading the metal ions into other materials, such as zeolites, and then loading the composite material as particulate fillers into the polymer matrix is an effective method.[18,27,28] Zeolite, either natural (clinoptilolite, mordenite, and chabazite) or synthetic (A-type, X-type, and Y-type), is a kind of silicon aluminum acid salt, and pure zeolites have no antimicrobial activities.[27] On loading of Ag ions, which have the highest antibacterial property among the metal ions,[24] through the ion-exchange method, the as-prepared silver-exchanged zeolite (Ag-zeolite) antimicrobial agent develops a strong antibacterial property. Furthermore, Ag-zeolite possesses a high heat resistance and high stability and is nontoxic to humans; therefore, it has been used in toothbrushes, kitchen

Received: January 5, 2017
Accepted: March 16, 2017
Published: March 16, 2017

DOI: 10.1021/acsami.7b00230
ACS Appl. Mater. Interfaces XXXX, XXX, XXX−XXX

utensils, baby toys, and, of late, in medical instruments[18] as an antibacterial coating/ingredient.

In this article, we report an antibacterial composite film-based triboelectric nanogenerator (ACF-TENG) that utilizes Ag-zeolite/PP composite films as the triboelectric layer. The open-circuit voltage (V_{OC}), short-circuit current (I_{SC}), and transferred charge (Q_{Tr}) of the ACF-TENG are about 193.3, 225.4, and 233.3% of those of a pure PP film-based TENG, respectively. The composite films also exhibit excellent antibacterial properties against *Escherichia coli* as well as antifungal properties. These results provide a promising solution for self-powered electronics for healthcare.

2. RESULTS AND DISCUSSION

The fabrication process of the Ag-zeolite/PP composite thin film is environment-friendly and cost-effective, as schematically illustrated in Figure 1. The fabrication process includes four steps: materials mixing, film formation, film cutting, and ACF-TENG preparation. More details can be found in the Experimental Section. The ACF-TENG contains an Al (aluminum) foil as the electrode and the composite film as the triboelectric material.

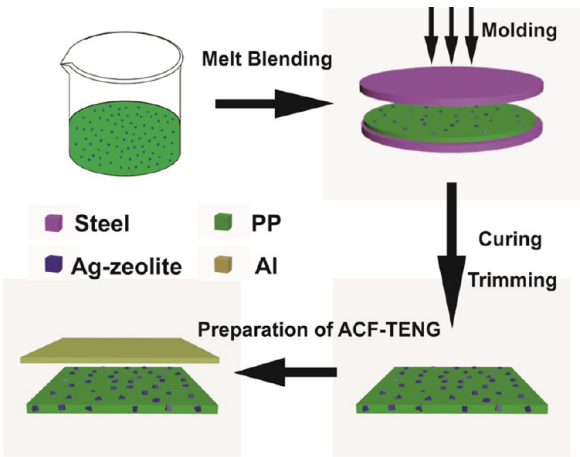

Figure 1. Schematic diagram of the process for fabricating a Ag-zeolite/PP composite film.

Figure 2a shows the X-ray diffraction (XRD) patterns of Ag-zeolite, a pure PP film, and the composite film. The peaks of Ag-zeolite are sharp and high, indicating that Ag-zeolite has good crystallinity. The three peaks contained by the rectangular are (3 1 1), (3 2 1), and (3 3 0), respectively. The diffraction patterns of the PP film show that the peaks are mostly sharp and high, indicating that the PP film has good crystallinity. The heights of the peaks of Ag-zeolite in the composite films become higher as the content increases from 1 to 5 wt %, as shown in the insert of Figure 2a. Therefore, the XRD results indicate that the Ag-zeolite particles are mixed well into the PP matrix.

Figure 2b shows the EDS patterns of Ag-zeolite, a pure PP film, and the composite films. There are no other elements observed in the pure PP film except carbon (C) and gold (Au) (Au came from the magnetron-sputtering process), which indicates the purity of the PP film. There are oxygen (O), sodium (Na), aluminum (Al), silicon (Si), and Ag in the Ag-zeolite. Here, C in the Ag-zeolite originates from the conductive carbon tape. The average proportion of Ag is about 1.5 wt %, and the proportion of Al is higher than that of the other elements, so Al can reveal the content change of Ag-zeolite in the composite films. With an increase in the Ag-zeolite content, the content of Al that came from Ag-zeolite also increased, implying that the Ag-zeolite particles are mixed in PP, which is in accord with the XRD results.

Figure 2c shows the FE-SEM images of the commercial Ag-zeolite particles, a pure PP film, and composite films. The insert shows an enlarged view of the FE-SEM image for the commercial Ag-zeolite without any further treatment. As can be seen, the Ag-zeolite particles are cubic, and the length of the edges is 2−3 μm. FE-SEM images of a pure PP film and composite films with an Ag-zeolite content ranging from 1 to 5 wt % indicate that there are no Ag-zeolite particles in the pure PP sample and the Ag-zeolite particles are on the surface or inlaid in the film. As the Ag-zeolite content increases, more Ag-zeolite particles can be observed in the FE-SEM images. In addition, the Ag-zeolite particles disperse evenly in the PP matrix for all samples.

On the basis of the prepared composite films, ACF-TENGs working in a single-electrode contact mode were fabricated with an Al foil as the electrode. The ACF-TENG forms a circuit through an external load of R between the Al foil and the ground, as shown in the inset of Figure 3a. To compare the triboelectric property of the composite films, TENGs using a pure PP film and composite films with the same size (2 × 2 cm^2) and thickness were fabricated and measured. Figure 3a presents the output voltage (V_{OC}) of the TENGs, exhibiting a pulse character. The positive and negative parts of the voltage of a pure PP film-based TENG are about 22.5 and 34.2 V, respectively, which are larger than those for a common single-electrode TENG.[29] For ACF-TENG, the negative part of the output voltage is almost the same as that of a pure PP film-based TENG because of the single-electrode structure of an ACF-TENG. As for the positive part, the voltage of the ACF-TENG increases by up to about 200% of that of the pure PP film-based TENG. The open-circuit voltage increases when Ag-zeolite is mixed in the films, but the average voltage remains almost the same as the Ag-zeolite content increases from 1 to 5 wt %. Figure 3c,e shows the short-circuit current and transferred charge of the TENGs, respectively, which show the same trend as the open-circuit voltage. The current and charge of the ACF-TENG are about 225.4 and 233.3% of those of the pure PP film-based TENG, respectively. Figure 3d,f shows the average current and transferred charge for 20 samples. The average values of I_{SC} and Q_{Tr} change slightly with an increase in the Ag-zeolite content.

The antibacterial effect of the pure PP film and composite films was obtained in a fluid nutrient medium using *E. coli*, which is the model of Gram-negative bacteria.[30,31] The films were cut into pieces with a diameter of ∼1 mm. The pieces (1 g) were added in 10 mL bacterium suspensions, with a concentration of about 10^5 CFU/mL. After co-culturing for 18 h at 37 °C in a shaker, 100 μL suspensions were then spread more or less uniformly on a Luria-Bertani (LB) agar culture medium in a large Petri dish (90 mm in diameter). Finally, the *E. coli* on the surface of the petri dish were collected and counted (Figure 4).

The antibacterial activity (R) was obtained using the following equation[19,20]

$$R = \frac{A - B}{A} \times 100\% \quad (1)$$

where A and B are the *E. coli* quantities on the surface of the sterile Petri dish that are poured from pure and composite PP particles, respectively. The number of *E. coli* colonies is counted and listed in Table 1.

Table 1 shows the antibacterial efficiency of the films. A pure PP film has no antibacterial efficiency. After filling with Ag-zeolite

DOI: 10.1021/acsami.7b00230
ACS Appl. Mater. Interfaces XXXX, XXX, XXX−XXX

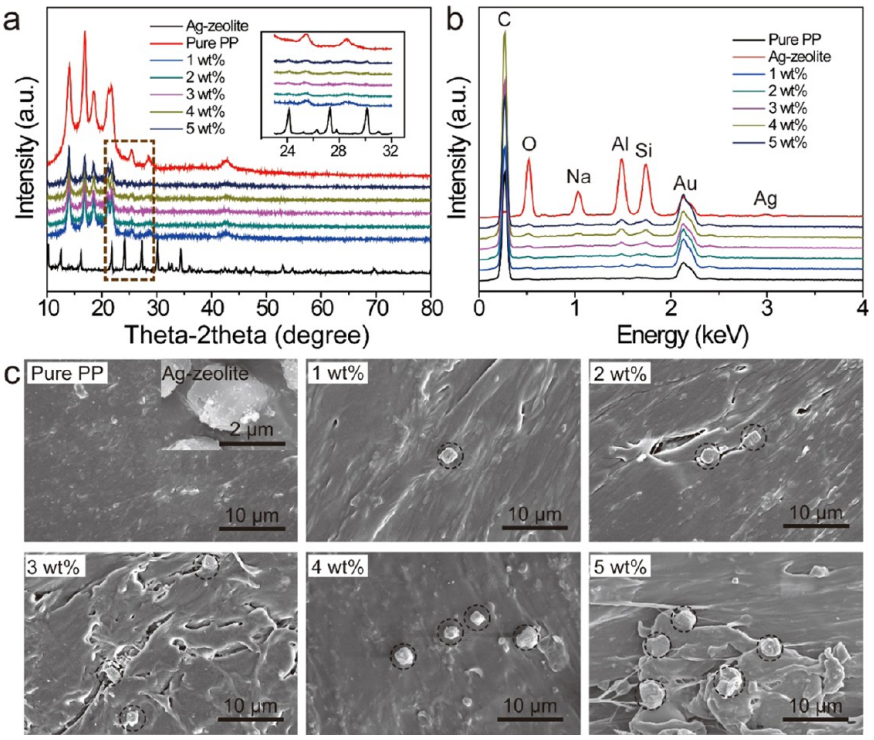

Figure 2. (a) XRD patterns of Ag-zeolite and the composite films. (b) Energy-dispersive spectral (EDS) patterns of Ag-zeolite and the composite films. (c) Field-emission scanning electron microscopy (FE-SEM) images of a pure PP film and the composite films; the insert of the pure PP image is the image of Ag-zeolite.

agents, the antibacterial efficiency increases as the Ag-zeolite content increases. When the added amount is 1 wt %, the antibacterial efficiency can reach 99.95%, demonstrating the high antibacterial activity of Ag-zeolite. When the weight ratio of the Ag-zeolite reaches 2%, the antibacterial efficiency reaches 99.99%. As the Ag-zeolite keeps increasing, the antibacterial efficiency remains constant at 100%. The results show that the composite films with a Ag-zeolite weight ratio higher than 2% have excellent antibacterial properties. The excellent antibacterial properties can be attributed to the silver ions, whose distribution in microbial cells disrupts the cell enzymatic activity,[18,28] and the higher the density of silver irons, the higher the antibacterial effect of the composite films. Therefore, the composite films with a Ag-zeolite ratio higher than 2 wt % are the optimized choice, considering the output performance of the ACF-TENGs and antibacterial properties of the composite films.

As mentioned above, the working mechanism of the ACF-TENG is based on triboelectrification and electrostatic induction.[32] On comparing the performances of ACF-TENGs and the pure PP film-based TENG, the open-circuit voltage, short-circuit current, and transferred charge of the ACF-TENGs are all found to be enhanced when Ag-zeolite particles are mixed into the PP film. To understand the role of Ag-zeolite particles mixed in the PP film, the dielectric permittivity (ε_r) of all of the films was tested. The dielectric permittivity of the composite films at room temperature is shown in Figure 5.

The dielectric permittivity of the composite films is minimum at a frequency of 100 kHz. At a fixed frequency, the value of ε_r increases as the Ag-zeolite content increases. From previous work,[32] the output voltage, V, can be expressed by

$$V = \frac{(\sigma_0 - \Delta\sigma)\cdot x(t)}{\varepsilon_0} - \frac{\Delta\sigma\cdot d}{\varepsilon_0\varepsilon_r} \quad (2)$$

where ε_0, ε_r, σ_0, and $\Delta\sigma$ are the vacuum permittivity, relative permittivity of the composite films, triboelectric charge density on the films, and transferred charge density on the Al electrode in a stage and $x(t)$, d, and t are the interlayer distance, thickness of the films, and time, respectively.

Under the open-circuit condition, the open-circuit voltage, V_{OC}, is given by[32]

$$V_{OC} = \frac{\sigma_0\cdot x(t)}{\varepsilon_0} \quad (3)$$

where ε_0, σ_0, and $x(t)$ are the vacuum permittivity, triboelectric charge density on the films, and interlayer distance, respectively. From eq 3, it seems that V_{OC} does not depend on the composite films. However, σ_0 is dependent on the capacitance of the device for a contact-mode generator because the generator acts as both an energy-storage and energy-output device.[33] The maximum capacitance (C_{max}) of the device is determined by

$$C_{max} = \varepsilon_0 S\cdot\frac{\varepsilon_r}{d} \quad (4)$$

Therefore, σ_0 is proportional to C_{max}, that is, proportional to ε_r/d. According to this understanding, the V_{OC} increases with an increase in the relative permittivity, ε_r, a decrease in the thickness of the composite films, or both. As shown in Figure 5, the dielectric permittivity of the composite films increases as the content of Ag-zeolite increases. Hence, the V_{OC} of the ACF-TENGs and the harvesting performance of the TENG improve.

As a further application, the ACF-TENG was integrated into insoles to realize healthy and wearable electronics. First, four springs were used to make sure that the composite film can separate from the Al electrode when the feet move upward, as shown in Figure 6c (the composite film has a size of 4 × 4 cm^2). Then, the ACF-TENG was seamed into the insoles and put into

DOI: 10.1021/acsami.7b00230
ACS Appl. Mater. Interfaces XXXX, XXX, XXX−XXX

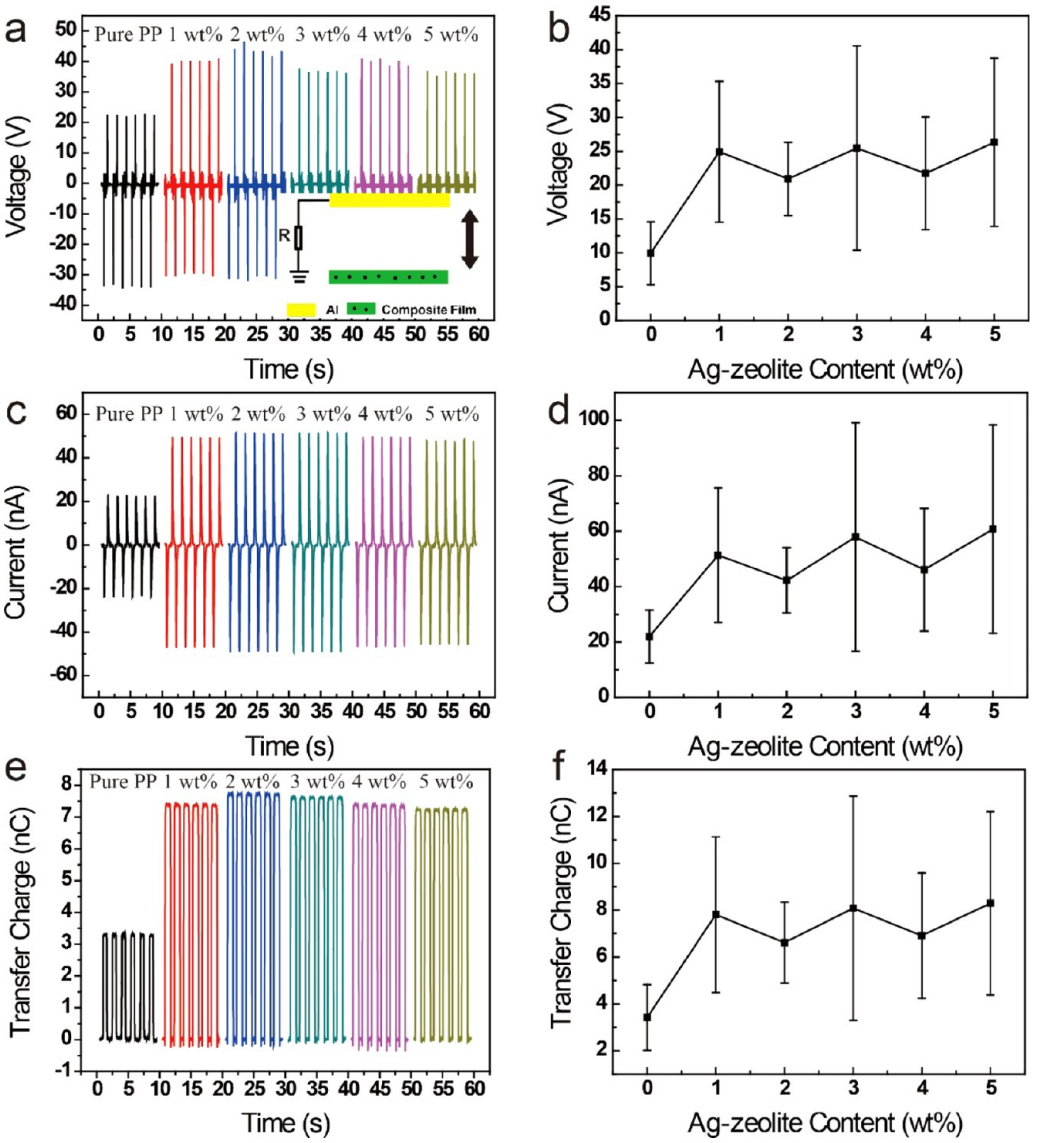

Figure 3. Output signals of the ACF-TENGs. (a), (c), and (e) show the V_{OC}, I_{SC}, and Q_{Tr}, respectively. The insert of (a) is the schematic diagram of the TENG. (b), (d), and (f) show the corresponding error bars of V_{OC}, I_{SC}, and Q_{Tr}, respectively.

the shoes (Figure 6a,b). As shown in Figure 6f, the V_{OC} of the ACF-TENGs with pure PP and with 2 wt % Ag-zeolite composite films are respectively about 150 and 300 V. Figure 6d shows that the ACF-TENG can light up five green light-emitting diodes (LEDs) when the terminal of the LED is connected to the ground. Through rectification of the alternating-current output, the direct-current output can be stored in energy-storage devices, such as capacitors. As shown in Figure 6g, the voltage of the 1 μF capacitor is 10 and 12 V when powered by the pure PP-based TENG and the ACF-TENG with the 2 wt % Ag-zeolite composite film for 5 min, respectively. The capacitor (1 μF) charged by the ACF-TENG can also light up five green LEDs (shown in Figure 6e), and the LEDs are brighter than the ones lit up by only the ACF-TENG. After the insoles were worn for 100 h, antibacterial tests were performed. The athlete's foot fungus is a kind of fungus, so the composite films were cultured in a fungus culture medium. The results are shown in Figure 6h,i. There were only a few fungal colonies on the 2 wt % zeolite composite film. Compared to the number of colonies on the pure PP film, the number of colonies on the 2 wt % zeolite composite film was almost negligible, which shows the good antifungal activity of the composite film and improves its feasibility for use in insoles.

3. CONCLUSIONS

In summary, an ACF-TENG was fabricated using Ag-zeolite/PP composite films as the triboelectric layer. By adding Ag-zeolite, the dielectric permittivity and surface charge density of the films were increased, which improved the performance of the ACF-TENG notably. The open-circuit voltage, short-circuit current, and transferred charge of the ACF-TENG are about 193.3, 225.4, and 233.3% of those of the pure PP film-based TENG, respectively. Because of the Ag ions, the ACF-TENG has excellent antibacterial and antifungal properties, through which over 99.99% of the bacteria and fungi can be killed. Integrating ACF-TENGs into insoles can not only lead to harvesting of walking energy to generate electricity but can also lead to effective elimination of the athlete's foot fungus. This work may help find a brand new approach to designing and fabricating new antibacterial and self-powered healthcare electronics based on TENGs.

DOI: 10.1021/acsami.7b00230
ACS Appl. Mater. Interfaces XXXX, XXX, XXX−XXX

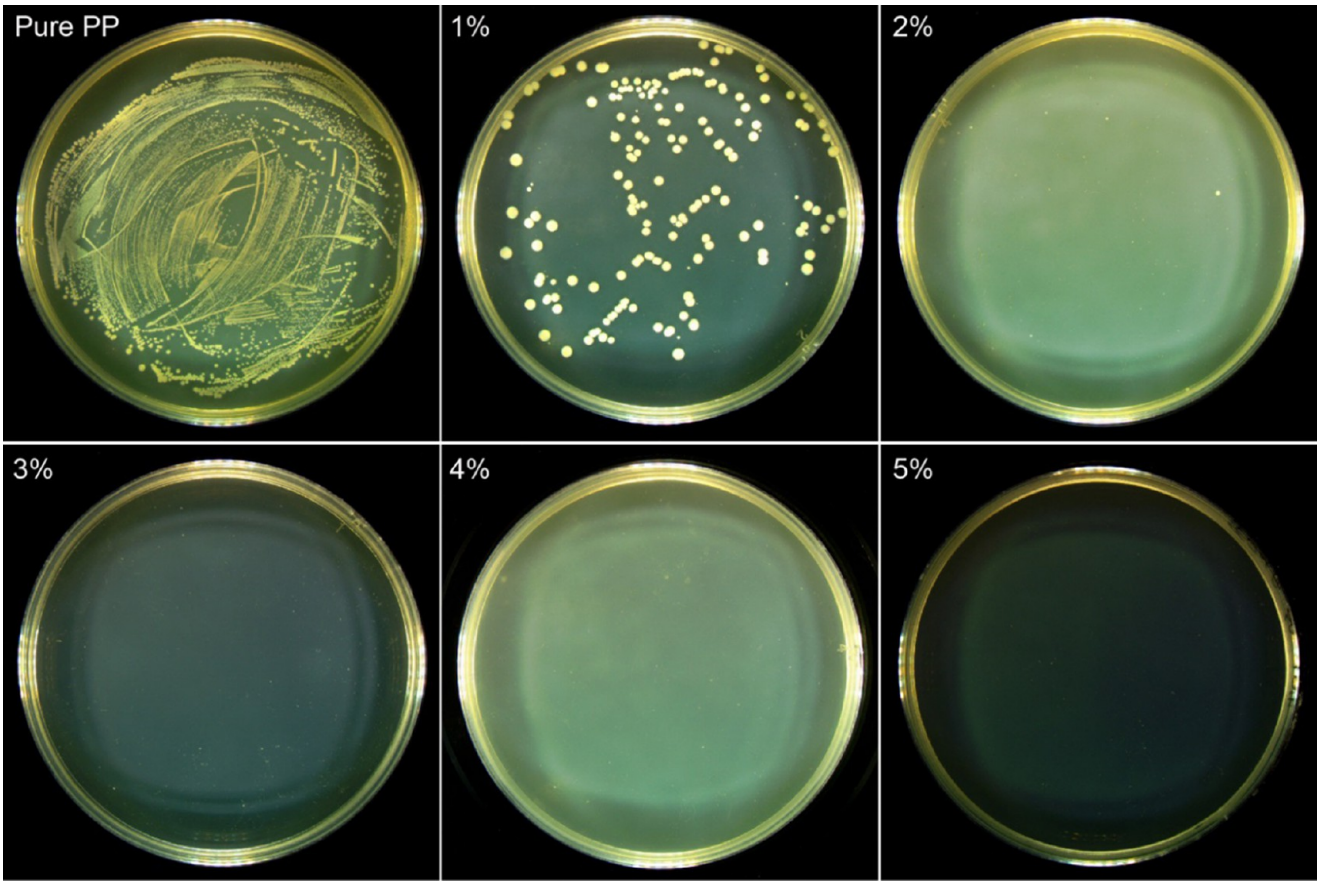

Figure 4. Photographs of *E. coli* colonies after co-culturing for 18 h with the composite samples.

Table 1. Antibacterial Efficiency of the Composite Films

composite film	pure PP	1 wt %	2 wt %	3 wt %	4 wt %	5 wt %
E. coli number after 18 h	334×10^3	181	1	0	0	0
antibacterial efficiency	none	99.95%	99.99%	100%	100%	100%

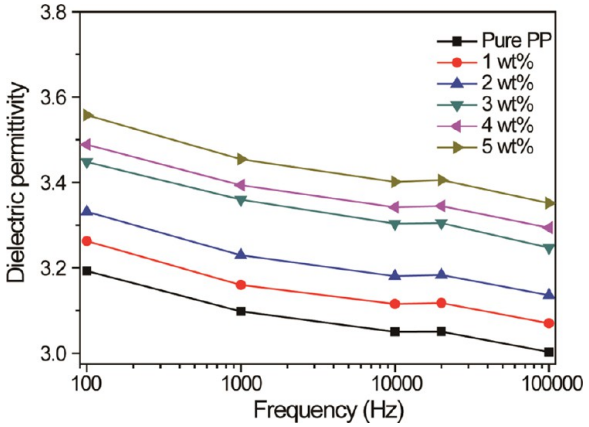

Figure 5. Dependence of the dielectric permittivity of the composite films on frequency at room temperature.

4. EXPERIMENTAL SECTION

4.1. Fabrication of PP Composite Films with Ag-Zeolite and a TENG. Commercially available Ag-zeolite and PP particles were used to fabricate the composite films. First, PP particles and Ag-zeolite were mixed through mechanical agitation until they were fully mixed. Then, they were melt-blended at a temperature of 210 °C in a N_2 atmosphere to avoid oxidation and mixed through mechanical agitation. Then, the compound was poured into a flat mold, heated to 215 °C, kept for 10 min at this temperature, and then cooled naturally to room temperature. Thereafter, the composite films were cut into pieces of 2×2 cm^2 and assembled as a single-electrode contact TENG.

4.2. Characterization and Measurements. The morphology and structural properties were examined by FE-SEM (Quanta 450 FEG, FEI) and XRD (PANalytical X'Pert3 Powder, The Netherlands). The chemical composition and element distribution were examined by an energy-dispersive X-ray spectroscope assembled on the FE-SEM. The open-circuit voltage, short-circuit current, and transferred charge of the TENG were tested with an oscilloscope (DSO-X 2014A; Agilent), a low-noise current amplifier (model no. SR570; Stanford Research Systems, Inc.), and a system electrometer (6514; Keithley), respectively.

4.3. Antibacterial Test. A fresh bacterial solution was first acquired by culturing *E. coli* in autoclaved LB broth at 37 °C for 24 h after inoculation (bacteria were in the stationary phase); the rotation speed was 120 rpm. Thereafter, the bacterial solution was centrifuged at 10 000 rpm to separate the bacteria from the culture medium, and then, the bacteria were washed and resuspended in sterilizing saline to reach a concentration of about 10^5 CFU/mL for the sterilization test.

4.4. Dielectric Permittivity Test. The dielectric permittivity of the composite films was tested using an LCR meter (4263B; Agilent). First, the composite films were deposited on Al electrodes through magnetron sputtering, forming a parallel-plate capacitor. The capacitances were tested under different frequencies (100 Hz and 1, 10, 20, and 100 kHz).

DOI: 10.1021/acsami.7b00230
ACS Appl. Mater. Interfaces XXXX, XXX, XXX−XXX

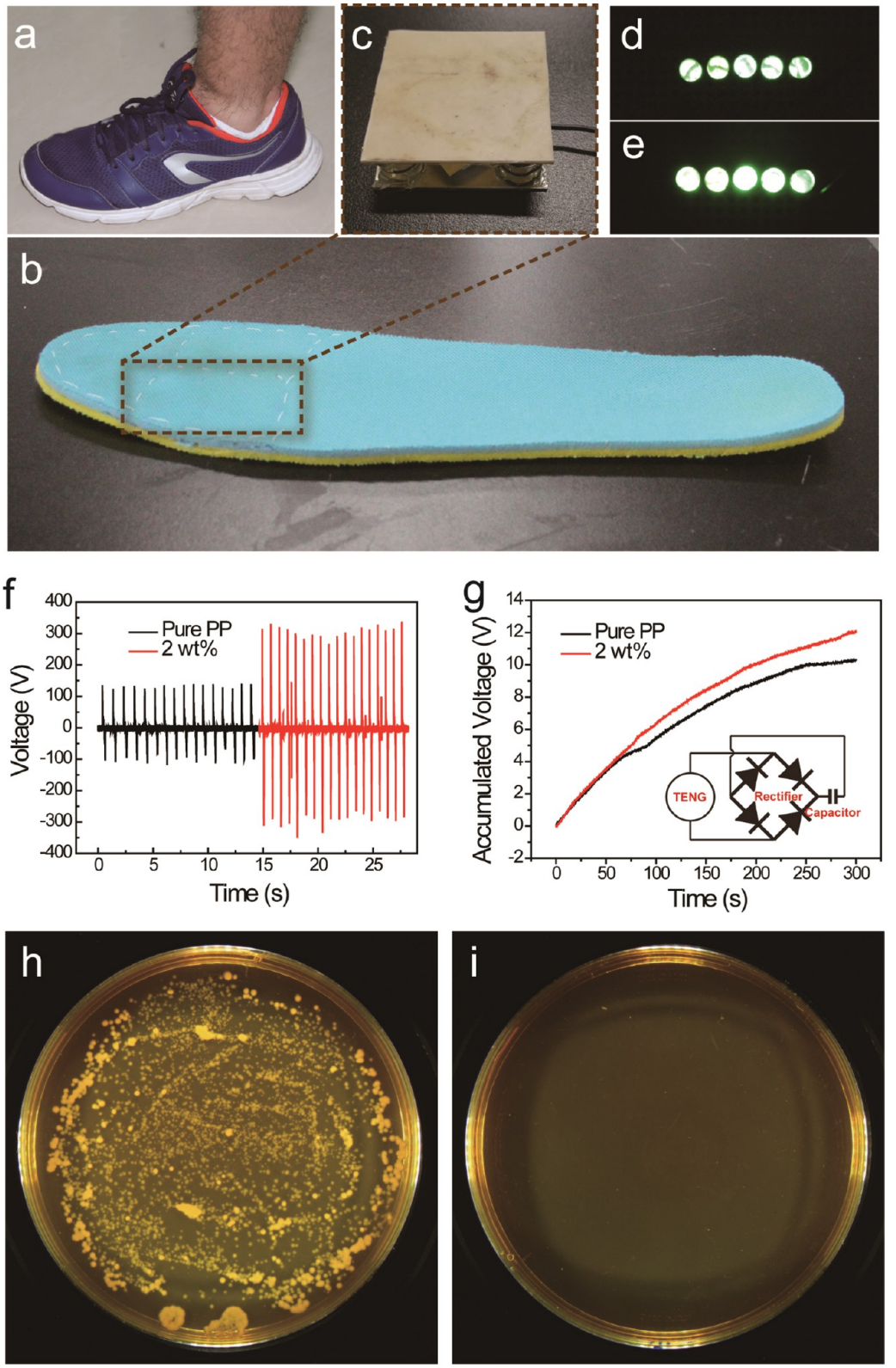

Figure 6. (a–c) ACF-TENG used in insoles. (d) Photograph of a lighting panel of five green LEDs driven by the ACF-TENG. (e) Photograph of a lighting panel of five green LEDs driven by the capacitor that was charged with the ACF-TENG. (f) V_{SC} of the ACF-TENGs used in insoles. (g) Accumulated voltage across a single capacitor (1 μF) charged with the ACF-TENG. (h, i) Photographs of ACF-TENGs with the pure PP and 2 wt % Ag-zeolite composite PP film, respectively.

The capacitances were used to calculate the dielectric permittivities of the composite films through the parallel-plate capacitor formula.

AUTHOR INFORMATION

Corresponding Authors
*E-mail: zli@binn.cas.cn (Z.L.).

DOI: 10.1021/acsami.7b00230
ACS Appl. Mater. Interfaces XXXX, XXX, XXX–XXX

*E-mail: zlwang@gatech.edu (Z.L.W.).

ORCID

Zhou Li: 0000-0002-9952-7296

Zhong Lin Wang: 0000-0002-5530-0380

Author Contributions

‖G.Q.G., C.B.H., and J.J.T. contributed equally to this work.

Notes

The authors declare no competing financial interest.

■ ACKNOWLEDGMENTS

Support from the "thousands talents" program for the pioneer researcher and his innovation team, the National Key R & D Project from the Minister of Science and Technology (2016YFA0202704), the National Natural Science Foundation of China (grant no. 51432005, 51608039, 5151101243, and 51561145021), and the Natural Science Foundation of Beijing, China (grant no. 4154090), is appreciated.

■ REFERENCES

(1) Xie, Y.; Wang, S.; Lin, L.; Jing, Q.; Lin, Z.-H.; Niu, S.; Wu, Z.; Wang, Z. L. Rotary Triboelectric Nanogenerator Based on a Hybridized Mechanism for Harvesting Wind Energy. *ACS Nano* **2013**, *7*, 7119−7125.

(2) Yang, Y.; Zhu, G.; Zhang, H. L.; Chen, J.; Zhong, X. D.; Lin, Z. H.; Su, Y. J.; Bai, P.; Wen, X. N.; Wang, Z. L. Triboelectric Nanogenerator for Harvesting Wind Energy and as Self-Powered Wind Vector Sensor System. *ACS Nano* **2013**, *7*, 9461−9468.

(3) Wang, S.; Mu, X.; Wang, X.; Gu, A. Y.; Wang, Z. L.; Yang, Y. Elasto-Aerodynamics-Driven Triboelectric Nanogenerator for Scavenging Air-Flow Energy. *ACS Nano* **2015**, *9*, 9554−9563.

(4) Zhao, Z.; Pu, X.; Du, C.; Li, L.; Jiang, C.; Hu, W.; Wang, Z. L. Freestanding Flag-Type Triboelectric Nanogenerator for Harvesting High-Altitude Wind Energy from Arbitrary Directions. *ACS Nano* **2016**, *10*, 1780−1787.

(5) Lin, Z. H.; Cheng, G.; Wu, W. Z.; Pradel, K. C.; Wang, Z. L. Dual-Mode Triboelectric Nanogenerator for Harvesting Water Energy and as a Self-Powered Ethanol Nanosensor. *ACS Nano* **2014**, *8*, 6440−6448.

(6) Su, Y. J.; Wen, X. N.; Zhu, G.; Yang, J.; Chen, J.; Bai, P.; Wu, Z. M.; Jiang, Y. D.; Wang, Z. L. Hybrid Triboelectric Nanogenerator for Harvesting Water Wave Energy and as a Self-Powered Distress Signal Emitter. *Nano Energy* **2014**, *9*, 186−195.

(7) Liang, Q.; Yan, X.; Gu, Y.; Zhang, K.; Liang, M.; Lu, S.; Zheng, X.; Zhang, Y. Highly Transparent Triboelectric Nanogenerator for Harvesting Water-Related Energy Reinforced by Antireflection Coating. *Sci. Rep.* **2015**, *5*, 9080.

(8) Hou, T. C.; Yang, Y.; Zhang, H. L.; Chen, J.; Chen, L. J.; Wang, Z. L. Triboelectric Nanogenerator Built Inside Shoe Insole for Harvesting Walking Energy. *Nano Energy* **2013**, *2*, 856−862.

(9) Zhu, G.; Bai, P.; Chen, J.; Wang, Z. L. Power-Generating Shoe Insole Based on Triboelectric Nanogenerators for Self-Powered Consumer Electronics. *Nano Energy* **2013**, *2*, 688−692.

(10) Zheng, Q.; Shi, B. J.; Fan, F. R.; Wang, X. X.; Yan, L.; Yuan, W. W.; Wang, S. H.; Liu, H.; Li, Z.; Wang, Z. L. In Vivo Powering of Pacemaker by Breathing-Driven Implanted Triboelectric Nanogenerator. *Adv. Mater.* **2014**, *26*, 5851−5856.

(11) Fan, F.-R.; Tian, Z.-Q.; Wang, Z. L. Flexible Triboelectric Generator! *Nano Energy* **2012**, *1*, 328−334.

(12) Bai, P.; Zhu, G.; Lin, Z. H.; Jing, Q. S.; Chen, J.; Zhang, G.; Ma, J.; Wang, Z. L. Integrated Multi Layered Triboelectric Nanogenerator for Harvesting Biomechanical Energy from Human Motions. *ACS Nano* **2013**, *7*, 3713−3719.

(13) Lin, Z. H.; Cheng, G.; Yang, Y.; Zhou, Y. S.; Lee, S.; Wang, Z. L. Triboelectric Nanogenerator as an Active UV Photodetector. *Adv. Funct. Mater.* **2014**, *24*, 2810−2816.

(14) Zheng, Y. B.; Cheng, L.; Yuan, M. M.; Wang, Z.; Zhang, L.; Qin, Y.; Jing, T. An Electrospun Nanowire-Based Triboelectric Nanogenerator and Its Application in a Fully Self-Powered UV Detector. *Nanoscale* **2014**, *6*, 7842−7846.

(15) Chen, J.; Zhu, G.; Yang, W. Q.; Jing, Q. S.; Bai, P.; Yang, Y.; Hou, T. C.; Wang, Z. L. Harmonic-Resonator-Based Triboelectric Nanogenerator as a Sustainable Power Source and a Self-Powered Active Vibration Sensor. *Adv. Mater.* **2013**, *25*, 6094−6099.

(16) Zhu, Y.; Yang, B.; Liu, J.; Wang, X.; Wang, L.; Chen, X.; Yang, C. A Flexible and Biocompatible Triboelectric Nanogenerator with Tunable Internal Resistance for Powering Wearable Devices. *Sci. Rep.* **2016**, *6*, 22233.

(17) Zhou, T.; Zhang, C.; Han, C. B.; Fan, F. R.; Tang, W.; Wang, Z. L. Woven Structured Triboelectric Nanogenerator for Wearable Devices. *ACS Appl. Mater. Interfaces* **2014**, *6*, 14695−14701.

(18) Pehlivan, H.; Balkose, D.; Ulku, S.; Tihminlioglu, F. Characterization of Pure and Silver Exchanged Natural Zeolite Filled Polypropylene Composite Films. *Compos. Sci. Technol.* **2005**, *65*, 2049−2058.

(19) Li, M.; Li, G.; Jiang, J.; Tao, Y.; Mai, K. C. Preparation, Antimicrobial, Crystallization and Mechanical Properties of Nano-ZnO-supported Zeolite Filled Polypropylene Random Copolymer Composites. *Compos. Sci. Technol.* **2013**, *81*, 30−36.

(20) Jiang, J.; Li, G.; Ding, Q.; Mai, K. C. Ultraviolet Resistance and Antimicrobial Properties of ZnO-Supported Zeolite Filled Isotactic Polypropylene Composites. *Polym. Degrad. Stab.* **2012**, *97*, 833−838.

(21) Erem, A. D.; Ozcan, G.; Skrifvars, M. In Vitro Assessment of Antimicrobial Polypropylene/Zinc Oxide Nanocomposite Fibers. *Text. Res. J.* **2013**, *83*, 2152−2163.

(22) Li, M.; Li, G.; Jiang, J.; Zhang, Z. S.; Dai, X.; Mai, K. C. Ultraviolet Resistance and Antimicrobial Properties of ZnO in the Polypropylene Materials: A Review. *J. Mater. Sci. Technol.* **2015**, *31*, 331−339.

(23) Li, X.; Pi, L.; Nie, M.; Wang, Q. Joint Effects of Rotational Extrusion and TiO_2 on Performance and Antimicrobial Properties of Extruded Polypropylene Copolymer Pipes. *J. Appl. Polym. Sci.* **2015**, *132*, No. 42410.

(24) Klasen, H. J. A Historical Review of the Use of Silver in the Treatment of Burns. II. Renewed Interest for Silver. *Burns* **2000**, *26*, 131−138.

(25) Fages, E.; Pascual, J.; Fenollar, O.; Garcia-Sanoguera, D.; Balart, R. Study of Antibacterial Properties of Polypropylene Filled with Surfactant-Coated Silver Nanoparticles. *Polym. Eng. Sci.* **2011**, *51*, 804−811.

(26) Palza, H.; Quijada, R.; Delgado, K. Antimicrobial Polymer Composites with Copper Micro- and Nanoparticles: Effect of Particle Size and Polymer Matrix. *J. Bioact. Compat. Polym.* **2015**, *30*, 366−380.

(27) İyigündoğdu, Z. U.; Demirci, S.; Bac, N.; Sahin, F. Development of Durable Antimicrobial Surfaces Containing Silver- and Zinc-Ion-Exchanged Zeolites. *Turk. J. Biol.* **2014**, *38*, 420−427.

(28) Boschetto, D. L.; Lerin, L.; Cansian, R.; Pergher, S. B. C.; Di Luccio, M. Preparation and Antimicrobial Activity of Polyethylene Composite Films with Silver Exchanged Zeolite-Y. *Chem. Eng. J.* **2012**, *204−206*, 210−216.

(29) Yi, F.; Lin, L.; Niu, S. M.; Yang, J.; Wu, W. Z.; Wang, S. H.; Liao, Q. L.; Zhang, Y.; Wang, Z. L. Self-Powered Trajectory, Velocity, and Acceleration Tracking of a Moving Object/Body Using a Triboelectric Sensor. *Adv. Funct. Mater.* **2014**, *24*, 7488−7494.

(30) Pline, W. A.; Lacy, G. H.; Stromberg, V.; Hatzios, K. K. Antibacterial Activity of the Herbicide Glufosinate on Pseudomonas Syringae Pathovar Glycinea. *Pestic. Biochem. Physiol.* **2001**, *71*, 48−55.

(31) de Oliva Neto, P.; Ferreira, M. A.; Yokoya, F. Screening for Yeast with Antibacterial Properties from an Ethanol Distillery. *Bioresour. Technol.* **2004**, *92*, 1−6.

(32) Niu, S. M.; Wang, S. H.; Lin, L.; Liu, Y.; Zhou, Y. S.; Hu, Y. F.; Wang, Z. L. Theoretical Study of Contact-Mode Triboelectric Nanogenerators as an Effective Power Source. *Energy Environ. Sci.* **2013**, *6*, 3576−3583.

(33) He, X.; Guo, H.; Yue, X.; Gao, J.; Xi, Y.; Hu, C. Improving Energy Conversion Efficiency for Triboelectric Nanogenerator with Capacitor Structure by Maximizing Surface Charge Density. *Nanoscale* **2015**, *7*, 1896−1903.

DOI: 10.1021/acsami.7b00230
ACS Appl. Mater. Interfaces XXXX, XXX, XXX−XXX